JOURNAL OF MATERIALS SCIENCE 26 (1991) 484–490

Synthesis of "Stabilized $Mn_{1-x}Mg_xO$" system ($0.001 \leqslant x \leqslant 0.15$) and its structural, thermal, optical and magnetic studies

P. P. BAKARE, V. G. GUNJIKAR, C. E. DESHPANDE, S. K. DATE
Physical Chemistry Division, National Chemical Laboratory, Pune 411 008, India

A novel method of preparation, involving careful formation of a stoichiometric solid solution of stabilized $Mn_{1-x}Mg_xO$ system for eight different concentrations of x ($0.001 \leqslant x \leqslant 0.15$) is described. A variety of physicochemical techniques such as X-ray diffraction, DTA–TGA, reflectance spectra, magnetic susceptibility and XPS data are used to determine structure–property correlations in the solid solutions, which are (i) X-ray diffraction studies reveal the linear decrease of cubic lattice parameter with increasing x, (ii) DTA–TG–DTG studies which confirm the formation of solid solution and the stability of these solid solutions in air which increases from 515 to 565 K with x, (iii) the diffused reflectance spectra shows nearly perfect octahedral symmetry around Mn^{2+} ions, (iv) magnetic susceptibility data indicates the usual dilution effects of diamagnetic ions in antiferromagnetic host lattice, (v) XPS studies reveal the presence of mixed phase of Mn_2O_3–MgO on the surface which protects the bulk MnO from its further oxidation to higher oxides of manganese. This shows the important role of Mg^{2+} in the chemical passivation of manganous oxide.

1. Introduction

$Mn_{1-\delta}O$ is a well known member of the family of typical metal deficient monoxides of the 3d transition metal series which exhibits sodium chloride (B1) structure [1]. In an ideal stoichiometric composition, the cation has a bivalent oxidation state, this is seldom true. In other words, some extent of non-stoichiometry is always present due to metal deficiency, wherein $\delta = 0.001$ to 0.15, and clustering of charge compensating defects [2]. Extensive investigations have been focused on the following.

(i) The crystallographic structure below and above its Neel temperature [3].

(ii) Thermochemical effects and non-stoichiometry [4].

(iii) Defect structure [5] and related possible cluster models [6]. Per Kofstad [5] has reported that $Mn_{1-\delta}O$ has properties similar to Wustite, $Fe_{1-\delta}O$ and hence concluded that important cation defects are defect structures.

(iv) Electronic structure of stoichiometric as well as non-stoichiometric form [7–9].

(v) Spin–glass transitions [10, 11] around 40 K.

(vi) Its usefulness in the catalytic reactions [12, 13] of immense technological importance.

Manganous oxide is highly unstable even at room temperature in air. When it is exposed to air, even at normal conditions, it oxidizes further to black Mn_2O_3/MnO_2 and therefore difficult to handle for carrying out any solid state reactions. To overcome these difficulties, we have developed a superior chemical synthesis route to make stable manganous oxide by incorporating bivalent diamagnetic ions in the lattice. This variety of $Mn_{1-x}Mg_xO$ mixed oxide system is found to be stable in air up to 515 to 565 K and is easy to handle at room temperature. In a previous series of papers we reported extensive studies on synthesis and physicochemical characterization of $Mn_{1-x}Zn_xO$ system [14, 15] and its use in the preparation of Mn–Zn ferrites with high performance parameters [16–18].

As a continuation of the chemical passivation work on 3d transition metal monoxides [17, 18], we report in this paper (i) synthesis of eight different concentrations of $Mn_{1-x}Mg_xO$ ($0.001 \leqslant x \leqslant 0.15$) solid solutions, (ii) the stabilization and chemical passivation of unstable manganous oxide using Mg^{2+} ions and (iii) physico-chemical characterization in relation to their structural, thermal, optical and magnetic properties.

2. Experimental procedure

Eight different concentrations of $Mn_{1-x}Mg_xO$ ($0.001 \leqslant x \leqslant 0.150$) solid solutions were prepared by mixing homogeneously appropriate quantities of AR grade manganous and magnesium oxalates (prepared in the laboratory from AR grade chemicals and microanalysed), decomposing the mixture in a slow current of oxygen-free nitrogen around 1023 K for 4 h in a thoroughly tested silica-glass unit [15] capable of withstanding static vacuum (10^{-2} mm of Hg). The slow current of oxygen-free nitrogen is found necessary to take away the evolved gases such as CO, CO_2

0022–2461/91 $03.00 + .12

TABLE I Cubic lattice parameter a and thermal stability of $Mn_{1-x}Mg_xO$: DTA, TG, DTG study.

Magnesium concentration x in $Mn_{1-x}Mg_xO$	Cubic lattice parameter $a \pm 0.0003$ nm	Thermally stable in air up to ±5 K	Maximum oxygen uptake (%)			
			$MnO \rightarrow Mn_2O_3$		$MnO \rightarrow Mn_2O_3 \rightarrow Mn_3O_4$	
			up to 1130 K calculated	from TG	up to 1230 K calculated	from TG
0.001	0.4450	515	11.271	10.80	7.514	6.75
0.005	0.4450	545	11.245	10.80	7.497	6.85
0.010	0.4449	560	11.213	10.76	7.475	7.96
0.050	0.4439	565	10.950	10.70	7.300	8.23
0.100	0.4430	565	10.608	9.40	7.072	8.00
0.120	0.4426	565	10.466	9.30	6.978	8.10
0.130	0.4423	565	10.395	9.25	6.930	8.30
0.150	0.4419	565	10.249	9.15	6.833	8.35

and moisture formed during the decomposition of oxalates. Extra care is taken to remove the trace amounts of moisture and adsorbed gases. After the decomposition of oxalates is completed, the unit is tested for standing static vacuum. The furnace is switched off and the products are allowed to cool in static vacuum over about 12 h to room temperature. The resulting polycrystalline $Mn_{1-x}Mg_xO$ solid solutions were found to remain unchanged in colour. There is no indication of oxygen chemisorption leading to the immediate change in colour (from olive green to black). On the other hand, pure manganous oxide (olive green) reacts with oxygen at room temperature to form its higher oxides (black) by spontaneous exothermic reaction [19].

3. Physicochemical characterization

The polycrystalline solid solutions of $Mn_{1-x}Mg_xO$ ($0.001 \leqslant x \leqslant 0.15$) are characterized using a variety of analytical techniques.

Standard gravimetric methods of chemical analysis [20] are followed to determine the concentration of manganese and magnesium in $Mn_{1-x}Mg_xO$ system. Powder X-ray diffractograms for all solid solutions have been recorded using Philips 1730 X-ray diffractometer at room temperature. The cubic lattice parameter a is determined from the observed d values and the corresponding intensities. DTA–TG–DTG studies are carried out using MOM Derivatograph analyser (type 00-102) and Netzsch (STA 409) thermal analyser between room temperature to 1523 K in air and oxygen-free nitrogen atmosphere. Diffused reflectance spectra have been recorded on Pye Unicam SP8-300 UV-VIS spectrometer at room temperature. Magnetic susceptibility measurements are carried out using Cahn-electrobalance with liquid nitrogen cryostat assembly in the temperature range of 80 to 300 K, calibrated with $HgCo(SCN)_4$. X-ray photoelectron spectra are recorded on the calibrated VG Scientific ESCA-3 MK-II spectrometer with Al Kα radiation.

4. Results and discussions

Following well established protocols [20], accurate wet–gravimetric analyses have been performed to establish purity, homogeneity and stoichiometry of solid solutions. After establishing their identities, these polycrystalline materials have been subjected to measurements of their properties using different techniques. Powder X-ray diffractograms of all solid solutions of $Mn_{1-x}Mg_xO$ ($0.001 \leqslant x \leqslant 0.150$) have a characteristic pattern of single-phase rock-salt type crystal structure. Cubic lattice parameters of these solid solutions are derived from the careful and intensity wise analysis of X-ray diffractograms and presented in Table I. Fig. 1 shows the linear variation of cubic lattice parameter a with magnesium concentration (x) obeying Vegard's law [21]. The lattice parameter decreases linearly with increasing x. This variation can be clearly understood in terms of the substitutional occupancy of Mn^{2+} ions (ionic radius = 0.080 nm) by Mg^{2+} ions (ionic radius = 0.065 nm) in the lattice. Similar decreases have been earlier reported by Golikov *et al.* [22], Koltashkino *et al.* [23], Cheetham

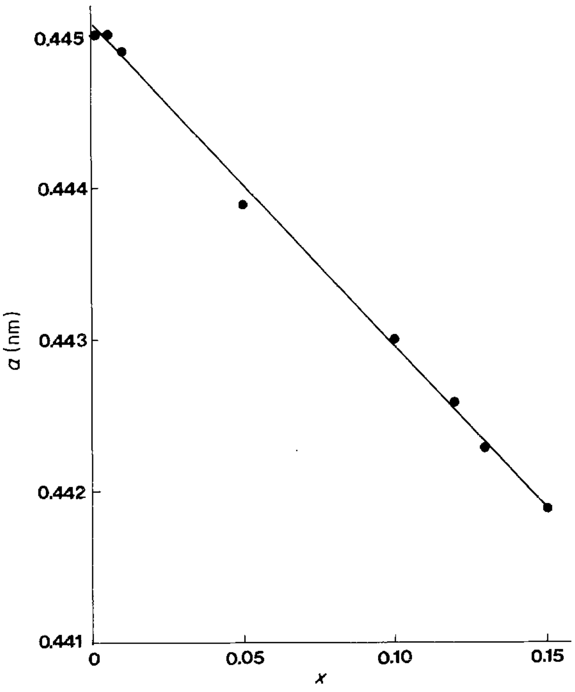

Figure 1 Variation of cubic lattice parameter with x. (in $Mn_{1-x}Mg_xO$)

TABLE II (a) DTA, TG, DTG studies of Manganous oxalate.
(b) DTA, TG, DTG studies of the formation of $Mn_{1-x}Mg_xO$ ($x = 0.001$)-system.

	Atmosphere	Reaction	Temperature (K)	Loss in weight (%)	Product
(a-i)	Oxygen-free nitrogen	Endothermic	411	19.57	Anhydrous oxalate
		Endothermic	687	59.43	Manganous oxide
(a-ii)	air	Endothermic	431	19.98	Anhydrous oxalate
		Exothermic	572	55.77	Mn_2O_3
		Endothermic	1200	57.26	Mn_3O_4
(b)	Oxygen-free nitrogen	Endothermic	413	19.18	Anhydrous manganous oxalate
		Endothermic	488	0.40	Anhydrous magnesium oxalate
		Endothermic	687	59.54	Manganous oxide
			771	0.14	Magnesium oxide

and Hope *et al.* [24], in ($Mn_{1-x}Ni_xO$) by Bakare *et al.* [25].

Thermal analysis of (i) manganous oxalate and (ii) magnesium oxalate has been reviewed by Duval [26] as follows.

(i) TG study indicates manganous oxalate, ($MnC_2O_4 \cdot 2H_2O$) being stable up to 327 K. It loses (two moles of) water of crystallization in the temperature range of 327 to 373 K. The anhydrous manganous oxalate remains stable up to 487 K which on further heating forms MnO around 553 K by losing CO and CO_2. MnO is found to be stable but later gains progressively in weight and is converted to Mn_2O_3 from 940 K.

(ii) TG study of magnesium oxalate ($MgC_2O_4 \cdot 2H_2O$) also indicated it to be stable up to 453 K. By losing two water molecules it forms an anhydrous salt in the temperature range of 453 to 523 K and remains stable from 523 to 673 K. On further heating it loses CO and CO_2 and forms MgO at 773 K. Both these oxalates do not form any carbonates during their thermal decomposition.

To confirm the formation of MnO and study of the possibility of its oxidation to higher oxides, DTA–TG–DTG study is carried out in slow current of (a-i) oxygen-free nitrogen and (a-ii) air in the temperature range of room temperature to 1523 K. The DTA–TG–DTG study of (a-i) showed that it dissociates by following two steps (Table II). At the first step, it loses two water molecules (wt loss = 19.57%) at 411 K and forms anhydrous oxalate. At the second step, it dissociates to manganous oxide at 687 K (wt loss = 59.43%). Both the steps are indicated by endothermic DTA peaks. The manganous oxide remains stable even upon further heating up to 1523 K as indicated by DTA–DTG–TG curves. On cooling to room temperature, the end product gets spontaneously oxidized to its higher oxides (black) in air. The results of this study agree well with those reported by Duval [26] except the progressive formation of Mn_2O_3 as seen in (a-i) above. The DTA–DTG–TG study carried out in (a-ii) air indicated that decomposition of oxalates in three steps (Table II). At the first step, it loses endothermally (DTA peak) two water molecules at 431 K (19.98% wt loss). At the second step, it further decomposes exothermally (DTA peak) and forms Mn_2O_3 at 572 K (55.77% wt loss) and in the third step, it is endothermally converted to Mn_3O_4 at 1200 K (57.26% wt loss). This indicates that even though MnO formation may have taken place, it is immediately oxidized to Mn_2O_3. It is now clear that for the formation of MnO from manganous oxalate, the decomposition has to be carried out in oxygen-free nitrogen. Next step is the study of formation of $Mn_{1-x}Mg_xO$ solid solution in oxygen-free nitrogen using manganese and magnesium oxalates by thermal analysis.

The DTA–TG–DTG study (b) of dissociation of oxalates of manganese and magnesium, mixed in appropriate proportions for $Mn_{1-x}Mg_xO$ solid solution with $x = 0.001$, is carried out in oxygen-free nitrogen. Fig. 2 shows four distinct endothermic DTA and DTG peaks around 413, 488, 687 and 771 K corresponding to loss of two water molecules of manganous oxalate, magnesium oxalate and dissociation of respective unhydrous oxalates to MnO and

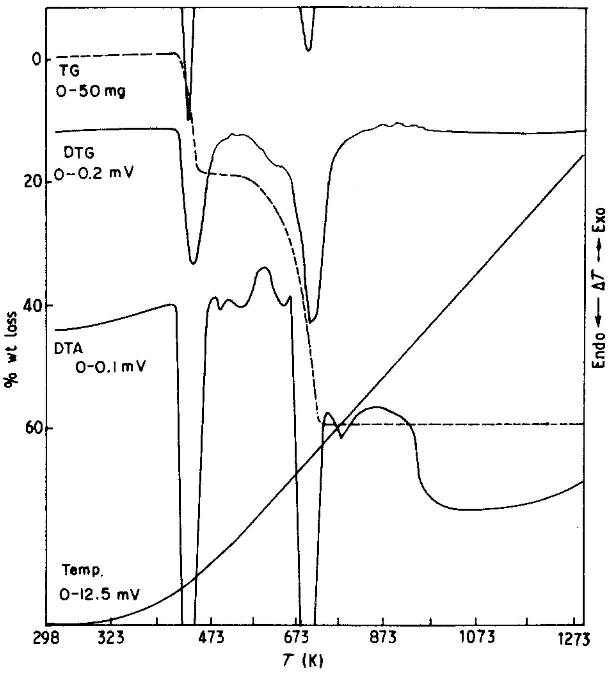

Figure 2 Thermogram of mixture of manganese and magnesium oxalates to study the formation of $Mn_{1-x}Mg_xO$ ($x = 0.001$) system.

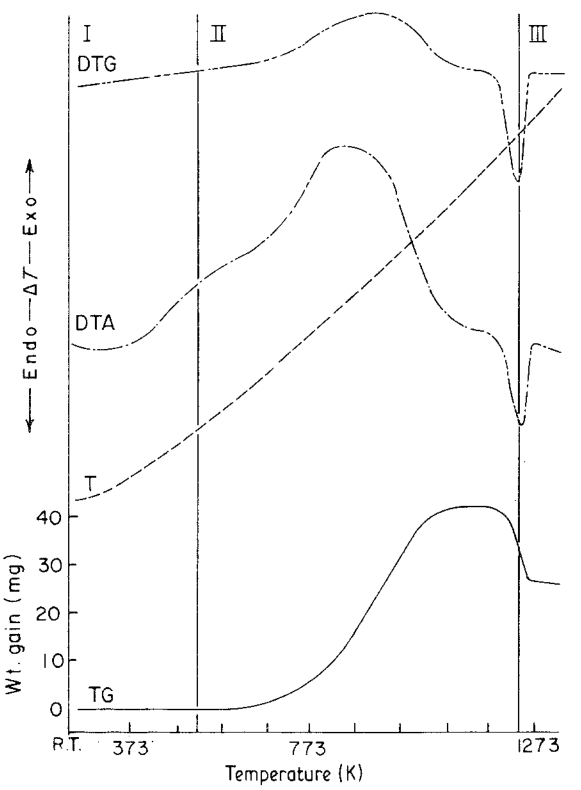

Figure 3 Thermogram of $Mn_{1-x}Mg_xO$ ($x = 0.001$) system.

MgO, respectively (Table II). MgO thus formed diffuses into MnO lattice and forms $Mn_{1-x}Mg_xO$ solid solution. To study (c) the thermal stability of the solid solutions and its dependence on magnesium concentration x in the system ($0.001 \leqslant x \leqslant 0.15$), DTA–TG–DTG curves are simultaneously recorded in the temperature range 295 to 1523 K in air. Fig. 3 shows the typical thermogram for the solid solution with lowest concentration of magnesium ($x = 0.001$). DTA curves shows three marked changes occurring in three temperature ranges (i) 295 to 515 K, (ii) 515–1130 K and (iii) 1130–1250 K. TG and DTG do not indicate any change or gain in weight to note the occurrence of any reaction. This behaviour can now be understood in terms of absence of any oxygen uptake. In contrast, it is well known that pure $MnO/Mn_{1-\delta}O$ system takes up oxygen spontaneously when exposed to air at room temperature [19]. It is clear that the $Mn_{1-x}Mg_xO$ ($x = 0.001$) system is chemically passivated and does not, therefore, pick up oxygen up to 515 K. In the temperature range II, the DTA curve shows a broad peak indicating a slow exothermic combustion type reaction; the TG curve indicates a continuous gain in weight of 10.8% up to 1130 K. This continuous gain is solely due to the uptake of oxygen and can be represented by the following thermochemical reaction

$$MnO \xrightarrow[\text{air}]{515\text{ K}} \text{stable} \xrightarrow[\text{air}]{1130\text{ K}} Mn_2O_3 \qquad (1)$$

The calculated gain in wt % for the slow oxidation reaction of $Mn_{1-x}Mg_xO$ system ($x = 0.001$) is 11.271% whereas the TG data shows it to be 10.8% in the temperature range II and remains constant. The observed lower oxygen uptake percentage in this case is due to the initial zero uptake of oxygen up to 515 K for $x = 0.001$. In other words, $x = 0.001$ system is thermally stable in air up to 515 K. In the temperature range III, DTA curve shows a sharp endothermic peak at $T \simeq 1230$ K which is accompanied by a loss in weight of 4.05% with a sharp DTG peak. The thermochemical reaction can be represented as

$$6Mn_2O_3 \xrightarrow[\text{air}]{1230\text{ K}} 4Mn_3O_4 + O_2 \qquad (2)$$

The calculated loss in wt % on the basis of this reaction is 3.757% for $x = 0.001$ system. Considering both the reactions 1 and 2 together, total gain in weight is 6.75% observed for $x = 0.001$ whereas the calculated gain in weight is 7.514%. This indicates that $Mn_{1-x}Mg_xO$ system ($x = 0.001$) takes up less oxygen or in other words is more stable in air than the pure $MnO/Mn_{1-\delta}O$ system. Similar behaviour is observed for other solid solutions with varying x. Table I gives the temperature at which oxygen uptake starts (indicating thermal stability in air) and comparative data of oxygen uptake, calculated and experimentally observed, for all the solid solutions. Table I also indicates that (i) highly unstable manganous oxide is stabilized even with such a low concentration of Mg^{2+} such as $x = 0.001$, (ii) the temperature at which oxygen uptake starts increases from 515 to 565 K with increasing concentration of magnesium.

4.1. Diffused reflectance spectroscopy

The diffused reflectance spectra of the solid solutions with $x = 0.01$, 0.05, 0.10 and 0.15 in $Mn_{1-x}Mg_xO$ system are recorded at room temperature in the range 380 to 760 nm (Fig. 4). In all the spectra, there are three distinct absorption peaks around 610 nm (16 395 cm^{-1}), 480 nm (20 835 cm^{-1}) and 420 nm (23 810 cm^{-1}). These observed peaks are assigned to $^6A_1 \rightarrow {}^4T_1$, $^6A_1 \rightarrow {}^4T_2$ and $^6A_1 \rightarrow 4_E$ transitions of $^6S_{5/2}$ ground state of Mn^{2+} ions on the basis of Tanabe–Sugano formalism [27]. These results (Table III) agree well with the earlier reported optical studies on single crystals of MnO by Pratt *et al.* [3], on $Mn_{1-x}Zn_xO$ system ($x = 0.001$ to 0.100) by Deshpande and Date [28] and also on $Mn_{1-x}Fe_xO$ system by Goodwin *et al.* [29]. It is thus possible to

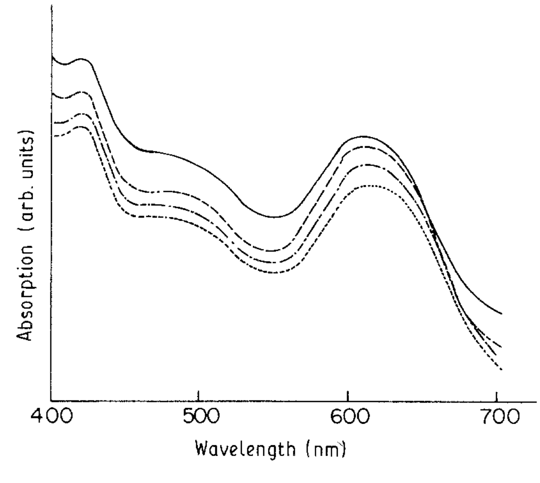

Figure 4 Reflectance spectra of $Mn_{1-x}Mg_xO$. (—— $x = 0.01$. --- $x = 0.05$, —·—·— $x = 0.10$, ------ $x = 0.15$).

TABLE III Optical absorption spectra of stabilized MnO stabilized with traces of MgO (concentration MgO $x = 0.01, 0.05, 0.10, 0.15$)

Frequency present work	Frequency Pratt and Coelho[13]	Assignments of the transitions from the ground state 6_{A_1}	Frequency (cm^{-1}) Deshpande *et al.*[28]
23810	23810	$4_{A_1}, 4_E$	23810
20835	20835	4_{T_2}	20835
16395	16395	4_{T_1}	16395

TABLE IV X-ray parameters and magnetic properties of $Mn_{1-x}M_xO$ compounds ($M = Mg^{2+}$).

x in $Mn_{1-x}Mg_xO$	a (nm) (± 0.0003)	μ_{eff} (BM)	θ (K)	T_{MIN} (K)
0.001	0.4450	5.82	573	120
0.005	0.4450	5.72	547	119
0.010	0.4449	5.73	568	118
0.050	0.4439	5.44	460	116
0.100	0.4430	5.44	440	114
0.120	0.4426	5.47	435	110
0.150	0.4419	5.45	445	100

see that Mn^{2+} ions in the $Mn_{1-x}Mg_xO$ system are present in near perfect octahedral symmetry. Presence of any appreciable change in the local orders and electronic structure of Mn^{2+} ions in the surrounding octahedra is ruled out as hardly any shift in the absorption peaks with increasing x is observed.

4.2. Magnetic susceptibility measurements

Magnetic susceptibility measurements of $Mn_{1-x}Mg_xO$ ($0.001 \leqslant x \leqslant 0.15$) have been carried out in the temperature range 77 to 300 K. The magnetic susceptibility of the sample is normalized for one gram atom of manganese and the plots of $1/\chi$ against T are given in Fig. 5 for various compositions. A broad minimum is seen in the plots at a temperature T_{MIN} (Minimum $1/\chi$ value) which is associated with the antiferromagnetic ordering temperature, T_N. The Weiss temperature, θ, is obtained by extrapolating the paramagnetic linear region of the $1/\chi$ against T plot to give an intercept on the temperature axis. In each case, the value of μ_{eff} is calculated from the slope of the curve above 200 K using least squares fit. The computed values of μ_{eff} are given in the Table IV. The observed values of T_N for $x = 0.001$ is nearly identical with the antiferromagnetic transition temperature of pure MnO, $T_N \simeq 120$ K [8, 9], indicating no change in the bulk magnetic properties arising due to long range ordering and exchange interactions. As the concentration of magnesium ions increases, the computed μ_{eff} value decreases from 5.82 to 5.45 BM and the sharpness of the inflection point decreases causing broadening of the minima (Fig. 4). In addition, T_{MIN} shifts to lower temperature from 120 to 100 K. The substitution of paramagnetic Mn^{2+} ions by diamagnetic Mg^{2+} ions affects the cooperative nature and the resulting exchange interactions amongst the magnetic ions. This is the usual dilution effect due to diamagnetic ions (wherein magnetic structure is broken into clusters with short range interactions). Similar dilution effects have been reported in the $Mn_{1-x}Zn_xO$ system [30].

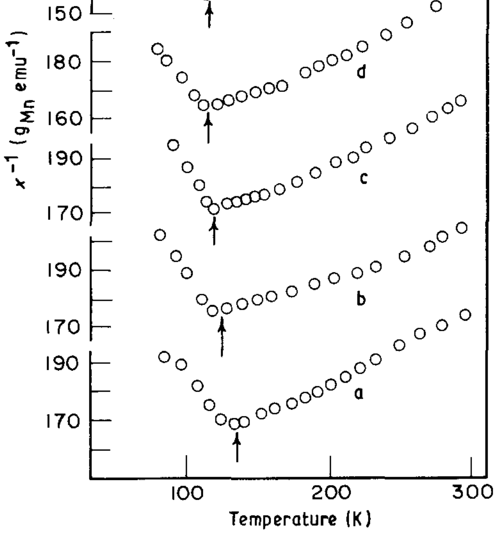

Figure 5 $1/\chi$ against T plots of $Mn_{1-x}Mg_xO$. (a $x = 0.001$, b $x = 0.005$, c $x = 0.01$, d $x = 0.05$, e $x = 0.10$, f $x = 0.12$).

Arkhipov [31] has reported the magnetic susceptibility of $Mn_xMg_{1-x}O$ system rich in magnesium, $0.027 \leqslant x \leqslant 0.30$ in the temperature range 80 to 800 K. It is also seen to obey Curie–Weiss law and magnetic moments are consistent with those expected from $^6S_{5/2}$ ground state of Mn^{2+} ions.

4.3. X-ray photoelectron spectroscopy (XPS)

Recently, Deshpande *et al.* [32] have reported thermogravimetric and XPS studies on stabilized $Mn_{1-x}Zn_xO$ ($x = 0.001$). They have proposed that MnO is stabilized with the small concentration of Zn^{2+} ions present on the surface in the form Mn_2O_3–ZnO mixed phase. To understand the passivation process and to establish the presence of a similar mixed phase on the surface of $Mn_{1-x}Mg_xO$ system, XPS studies have been carried out at room temperature and high temperature, $T \simeq 573$ K.

As stated earlier, X-ray photoelectron spectra of samples with $x = 0.001, 0.01$ are recorded using an Al Kα radiation source (1486.6 eV). Initially, full-general scans (1000 eV) are recorded to check all appropriate peaks corresponding to the expected chemical composition on the surface. Fig. 6 shows high resolution XPS scans recorded over a narrower energy scale (100 eV) for the samples with $x = 0.001$

TABLE V XPS data on $Mn_{1-x}Mg_xO$ system with $x = 0.001$ and 0.01 (before and after heating at 573 K for 2 h in air)

x (in $Mn_{1-x}Mg_xO$)	Binding energy (BE) eV ± 0.2 eV								
	Magnesium				Manganese				Oxygen, O^{--}
	$^1s_{1/2}$	$^2s_{1/2}$	^3p	^3s	ΔE^3s	$^2p_{3/2}$	$^2p_{1/2}$	ΔE^2p	^1s
0.001	1304	88.4	49.5	83.8	5.6	641.3	653.1	11.8	529.9
0.001 after heating at 573 K for 2 h in air.	1303	88.6	49.4	84.2	4.8	642.2	653.8	11.6	530.1
0.01	1304	88.4	48.80	83.8	5.8	641.5	653.5	12.0	529.8
0.01 after heating at 573 K for 2 h in air	1304	88.5	49.40	84.0	5.4	642.6	654.2	11.6	530.0

and 0.01, before and after the heating. High resolution scans were recorded for magnesium (1s, 2s), manganese (2s, 2p, 3s, 2p, 3d) and oxygen (1s, 2s, 2p) levels. Table V presents the XPS data, (before and after heating the samples in air) of characteristic peaks usually employed in assigning the oxidation states in transition metal oxides. From characteristic BE values ($2p_{3/2}$, $2p_{1/2}$, 3s) of Mn^{3+} in Mn_2O_3 [4, 32–37], the observed peaks are assigned to Mn^{3+} species present on the surface. At the same time, Mg^{2+} ions are also observed on the surface with high concentrations. The presence of Mg^{2+} and Mn^{3+} species on the surface indicates a possible formation of a mixed $MgO–Mn_2O_3$ phase. On heating the samples in air around 573 K i.e. temperature greater than the stabilization temperature recorded from DTA–TG–DTG studies, characteristic shifts in Mn(3s) levels are clearly observed. By comparing with the reported data [4, 35–37] of shifts in Mn-O system, these peaks are assigned to Mn^{4+} species on the surface. At the same time, Mg^{2+} (1s) peak is found to be very weak in intensity, implying the migration and/or diffusion of these species from the surface. Thus it is possible now to understand the stabilization process in terms of chemical passivation of the bulk MnO.

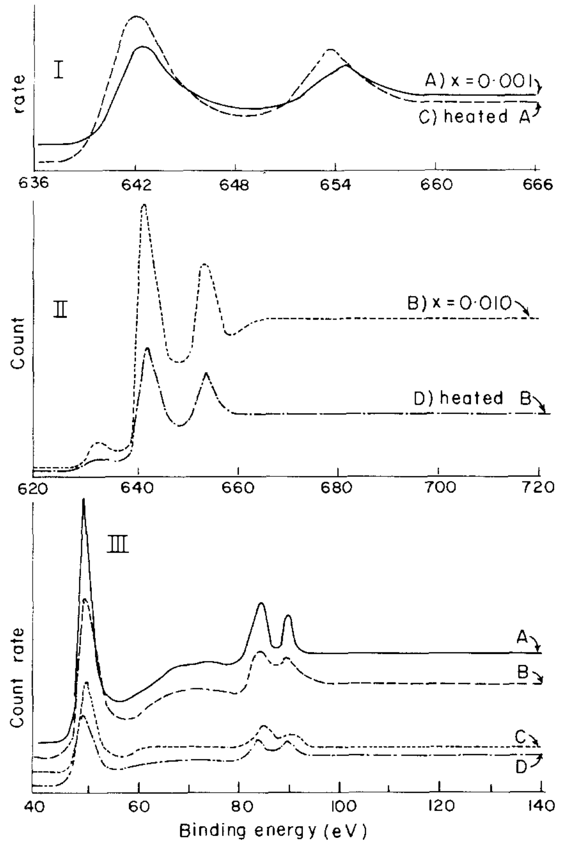

Figure 6 XPS of $Mn_{1-x}Mg_xO$.

Highly active sites (surface) are preferentially occupied by Mg^{2+} ions, which together with Mn^{3+} ions form a mixed phase $MgO–Mn_2O_3$. This surface phase prevents the subsequent oxidation of bulk MnO. Thermal treatment in air accelerates the migration/diffusion of Mg^{2+} ions, which in turn, reactivate the occupied active sites resulting in further oxidation of bulk MnO. These results are very similar to those reported earlier by Deshpande and Date [28] for $Mn_{1-x}Zn_xO$ system.

5. Conclusion

In summary, we have shown that stabilized solid solutions $Mn_{1-x}Mg_xO$ ($0.001 \leqslant x \leqslant 0.15$) system can be successfully prepared. X-ray diffraction studies reveal the formation of single cubic phase and linear decrease of the lattice parameter with increasing x (manganese concentration). DTA–TG–DTG studies clearly indicate the formation of solid solution and confirm their stability in air which increases from 515 to 565 K with increasing x. The diffused reflectance spectra clearly show the forbidden d–d transitions arising from the presence of Mn^{2+} ions in nearly perfect octahedral symmetry. Analysis of the magnetic susceptibility data of $Mn_{1-x}Mg_xO$ system show the usual dilution effects in antiferromagnetically ordered system. The presence of $Mn_2O_3–MgO$ (mixed phase on the surface of $Mn_{1-x}Mg_xO$) system prevents the subsequent oxidation of bulk MnO, as shown by XPS data. Stabilized $Mn_{1-x}Mg_xO$, with all these interesting properties, has been found useful in making high performance square-loop manganese and magnesium ferrites [38].

Acknowledgements

We are grateful to Dr P. Ratnasamy, FNA, Head, Physical Chemistry Division for his continued interests and encouragement for this work. Thanks are due to Mrs J. J. Shrotri for her generous help and to Mrs Nalini Jacob, Mr S. R. Padalkar, Mr J. S. Gujaral for their technical assistance in recording thermograms, reflectance spectra and X-ray diffractograms respectively. Thanks are also due to Drs S. Badrinarayanan and A. B. Mandale for recording XPS spectra.

References

1. C. N. R. RAO and G. V. SUBBA RAO, "Transition metal oxides", Nat. Standard Data Ser. (Nat. Bur. Stand, U.S., 1974).
2. A. Z. HED and D. S. TANNHAUSER, *J. Electrochem. Soc.* **114** (1967) 314.
3. C. W. PRATT and R. COELHO, *Phys. Rev.* **116** (1959) 281.
4. J. S. FOORD, R. B. JACKMAN and G. C. ALLEN, *Phil. Mag.* **A49** (1984) 657.
5. P. KOFSTAD, *J. Phys. Chem. Solids* **44** (1983) 879.
6. R. W. GRIMES, A. B. ANDERSON and A. H. HEUER, *J. Amer. Ceram. Soc.* **69** (1986) 619.
7. P. KOFSTAD, "Nonstoichiometry, Diffusion and electrical conductivity, Binary metal oxides" (Wiley, New York, 1972).
8. H. BIZETTE, C. F. SQUIREC and B. TSOU, *C.R. Acad. Sci.* **207** (1938) 449.
9. M. SEINO, J. MIYAHARA and Y. NOREY, *Phys. Lett.* **A44** (1973) 35.
10. J. J. HAUSER and J. V. WASZCZUK, *Phys. Rev.* **B30** (1984) 5167.
11. C. E. DESHPANDE, S. K. DATE and J. J. HAUSER, *J. Mater. Sci. Lett.* **5** (1986) 997.
12. G. C. MAITI, R. MALESA, U. LOCHNER, H. PAPP and M. BACRNS, *Appl. Catalysis* **16** (1985) 215.
13. M. A. BALTANAS, A. B. STILES and J. R. KATZER, *ibid.* **20** (1986) 31.
14. M. N. S. MURTHY, C. E. DESHPANDE, P. P. BAKARE and J. J. SHROTRI, Indian Patent 158 085 (1986).
15. C. E. DESHPANDE and M. N. S. MURTHY, *Bull. Mater. Sci.* (*Ind.*) **3** (1981) 261.
16. C. E. DESHPANDE, P. P. BAKARE and M. N. S. MURTHY, *Bull. Mater. Sci.* (*Ind.*) **5** (1983) 1.
17. C. E. DESHPANDE, PhD. Thesis, University of Poona, India (1985).
18. P. P. BAKARE, PhD Thesis, University of Poona, India (1985).
19. N. V. SIDGWICK, "Chemical elements and their compounds", Vol. II (Oxford, Clarendon, 1950), 1283.
20. A. I. VOGEL, "Quantitative Inorganic Analysis", 3rd Edn, (English Language Book Society, London, 1964).
21. E. F. KAELBLE (Ed.), "Handbook of X-rays" (McGraw Hill, New York, 1967). pp. 12–21.
22. Y. V. GOLIKOV and V. P. BARKHATOV, *Inorg. Mater.* **18** (1982) 1791.
23. S. T. KOLTASHKINA and G. V. PAPOV, *Chem. Abs.*, **70** (1969) 32265b.
24. A. K. CHEETHAM and D. A. O. HOPE, *Phys. Rev.* **B27** (1983) 6964.
25. P. P. BAKARE, C. E. DESHPANDE, J. J. SHROTRI, M. V. KUBER and S. K. DATE, Proceedings of 4th National Seminar on Physics of Semiconductors and Devices, edited by J. C. Gang and P. C. Mathur (1985), Jaipur, India, (1986) 273.
26. C. DUVAL, "Inorganic Thermogravimetric Analysis", 2nd Edn, (New York, Elsevier, 1963) p. 312.
27. F. A. COTTON and G. WILKINSON, "Advanced Inorganic Chemistry" (Wiley Interscience, New York 1962) p. 560.
28. C. E. DESHPANDE, S. BADRINARAYANAN and S. K. DATE, *J. Mater. Sci. Lett.* **3** (1984) 563.
29. C. A. GOODWIN, H. K. BROWN and D. ADLER, *Appl. Phys.* **45** (1974) 626.
30. C. E. DESHPANDE, P. P. BAKARE, M. N. S. MURTHY, N. Y. VASANTHACHARYA and P. GANGULY, *Proc. Ind. Acad. Sci.* (*Chem. Sci.*) **91** (1982) 261.
31. A. A. ARKHIPOV, *Chem. Abs.* **100** (1984) 149 798(g).
32. C. E. DESHPANDE, S. BADRINARAYANAN and S. K. DATE, *J. Mater. Sci. Lett.* **4** (1985) 922.
33. M. OKU, K. HIROKAWA and S. IKEDA, *J. Elect. Spectrosc. Rel. Phen.* **7** (1975) 465.
34. G. K. WERTHEIM, S. HUFNER and H. J. GUGGENHEIM, *Phys. Rev.* **B71** (1973) 556.
35. C. S. FADLEY and D. A. SHIRLEY, *Phys. Rev.* **A2** (1970) 1109.
36. C. N. R. RAO, D. D. SARMA, S. VASUDEVAN and M. S. HEGDE, *Proc. R. Soc.* **A367** (1979) 239.
37. J. C. CARVER, G. K. SCHWEITZER and T. A. CURLSON, *J. Chem. Phys.* **57** (1972) 973.
38. P. P. BAKARE, C. E. DESHPANDE, J. J. SHROTRI, M. P. GUPTA, S. K. DATE, *Ceram. Int.* **13** (1987) 247.

Received 25 September 1989
and accepted 9 March 1990.